CONSTRUCTION OF A ZIRCON- CEMENT PAD AND CALIBRATION OF PORTABLE SURVEY METERS FOR ENVIRONMENTAL RADIATION MEASUREMENTS

By

Habiba Altine Aliyu

(MSc./Sci./29834/2001-2002)

**Thesis submitted to the Postgraduate School,
Ahmadu Bello University, Zaria in partial fulfillment
of the Requirement for the Award of
Master of Science in Radiation Biophysics**

April 2006

DEDICATION

I dedicate this work to the Creator of everything and everyone, to my husband, Mallam Muhammadu Jibo, for his encouragement and support, to my sisters and my children for bearing with me throughout this exercise.

DECLARATION

I herby declare that the thesis entitled "**Construction of a Zircon - Cement Pad and Calibration of Portable Survey Meters for Environmental Radiation Measurements**" is my work. It has not been submitted for an award of degree or diploma to any other university or institution. Information derived from published and unpublished work of other researchers have been acknowledged and referenced.

_____ _____

Habiba Altine Aliyu Date

CERTIFICATION

This thesis titled "**Construction of a Zircon - Cement Pad and Calibration of Portable Survey Meters for Environmental Radiation Measurements"** meets the regulations governing the award of Masters of Science in Radiation Biophysics of the Ahmadu Bello University Zaria and is approved for its contribution to knowledge and literary presentation.

_____	_____
Dr.T.C.Akpa *Chairman, Supervisory Committee*	Date
_____	_____
Dr.S.P.Mallam *Member, Supervisory Committee*	Date
_____	_____
Prof. N.Hariharan *Head, Physics Department*	Date
_____	_____
Prof. J.U.Umoh *Dean, Postgraduate School*	Date

ACKNOWLEDGEMENTS

I have to express my immeasurable appreciation in acknowledging the invaluable contribution rendered to me especially by Dr. T. C.. Akpa and Dr. S. .P. Mallam, my supervisors, for their patience, encouragement, confidence and understanding, without such encouragement I would not have been able to see the end of this assignment. To Dr. I. .G. .E. Ibeanu, who was always ready to proffer useful suggestions. I also acknowledge and register my appreciation for the assistance and cooperation of all the Teaching and Technical Staff of Center for Energy Research and Training, Ahmadu Bello University Zaria, especially to Mallam .I. .A. Bappah for being ever ready to assist. I wish also to express my sincere appreciation to the Management of the Ahmadu Bello University Teaching Hospital, for sponsoring and giving me the opportunity to pursue the course. My appreciation also goes to the entire Members of Staff and Students of the School of Biomedical Engineering Technology, Ahmadu Bello University Teaching Hospital, Zaria, for their cooperation and assistance, especially Mr. O.A. Adetoye, the Head of Department for his magnanimity. I have to also thank the Heads, Physics Department, Dr. M. N. Umego, and Professor N. Hariharan as well as Engr. Bamgbelu and the Secretarial Staff of the Physics Department for their ready assistance. I must also register my profound gratitude to the entire members of my family including my friend and confidant, Talatu Danjuma for their support and encouragement. I could not complete without also acknowledging the useful suggestions and criticisms received from my colleagues, in and outside the course

Abstract

Zircon sand, a by-product of tin mining was collected from N'gell valley Tin Mining Company at 42km along Barikin Ladi road in Plateau State. The sand was characterized for activity content using NaI(Tl) scintillation detector. The activity of thorium in the zircon sand was 9726.151±20.16Bq/kg, while that of radium-was 538.848±10.08Bq/kg. The activity of cement was found to be very minimal with radium being 23.124±1.636Bq/kg, potassium 4.648±1.446Bq/kg and thorium 34.845±1.655Bq/kg. A ratio of two parts zircon sand to one part cement was thoroughly mixed with water to construct the calibration slab. Measurement of the activity over the slab from equidistant positions from the center shows that activity was uniformly distributed. The theoretical dose-rates at different heights from the center were calculated and were used to derive the calibration factor for different detectors available. The calibration factors for the three detectors are LUDLUM NaI(Tl) survey meter 0.509, X-ray and Gamma radiation ATK1120 0.233 and RDS-120 survey meter .39. The slab can be used as a calibration pad for calibrating survey meters for environmental radiation level measurements.

Table of Content

List of Tables

List of Figure

CHAPTER ONE

1.0 INTRODUCTION

Radioactivity could be defined as the spontaneous emission of ionizing particles or gamma rays when some nuclei known as radionuclides disintegrate. From time immemorial man has been exposed to natural radiation from the environment. There are two main sources of natural radiation; they are cosmic and terrestrial radiations. As a matter of fact, it is not possible to categorically say whether the natural background radiation has been beneficial or harmful to the development of the human species. What could be deduced is that a small but finite fraction of the natural mutations in cells must be beneficial since it leads to the evolution of higher life while on the other hand most of all genetic mutations lead to genetic defect and genetic death. It is obvious that these two effects have achieved some sort of balance since man has evolved to his present state despite background radiation or even because of it. (Alan and Harbison, 1988). Radiation, which reaches the earth from outer space, is known as cosmic radiation. The earth itself is radioactive and naturally occurring radionuclides are present in the air we breathe in, the food we eat, local effect, which exists as a result of human activity and in our bodies. This in effect means that everyone is exposed to natural radiation and in fact for most people it is the highest contributor.

The source of radiation exposure to man also known as natural radiation environment, consists of both internal and external sources. The most important internal sources are the radioactive elements ^{40}K and ^{222}Rn which are taken into the body. The external sources of exposure to man are cosmic and the naturally occurring radioactive isotopes of the ^{40}K, ^{238}U and ^{232}Th decay series. The internal

and external radiation level vary as a function of the geological formation, type of dwelling, in our bodies and local effect which exist as a result of human activity and elevation above sea level.

The disintegration of natural radioactive elements is accompanied by the emission of α and or β particles. The daughter nuclei then go into a state of excitation and the excess energy is emitted as gamma rays. Gamma rays have neither mass nor charge and they are more penetrating than α or β particles, as such they are used to characterize the terrestrial component of natural radiation environment. (IAEA, 1990). The gamma ray energy spectrum measured with gamma ray spectrometer can be used to determine the amounts of the different radioelements in a sample. This is determined by measuring the count rate in distinct energy windows specific for gamma ray energy of a particular element. Gamma ray spectrometry can be used in measuring the activity of natural radionuclides because the parent radionuclide is usually in secular equilibrium with their daughters. This is due to the fact that the parent radionuclides have very long half-lives in comparison with that of their daughters. As a result all the radionuclides of one decay chain have the same activity (IAEA,1990).

1.2 STATEMENT OF RESEARCH PROBLEM

Survey for radiation and airborne activity are performed to provide information on the current status of radiological conditions and it is also used for determining the protection requirements as a means of demonstrating compliance with regulation. As part of the research problems in environmental study, CERT has been characterizing the Jos Tin Mines tailings, which is highly radioactive. The need to measure radiation doses in-situ at the mining and processing sites has been felt for sometimes. For this to be done efficiently portable detectors have to be characterized and

calibrated for the measurements. Thus the mining samples have to be characterized and used in constructing calibration pad that can be used in calibrating detectors used as survey meters. Since air borne radioactivity can and does exist, whether naturally or by plant processes, it will be required that quantitative and qualitative measurements be made, in order to determine the concentration of radionuclides in the air to ensure that exposure are within limits, to estimate the extent of radiation level and hence enable monitoring of environmental releases.

1.3 OBJECTIVES OF THE RESEARCH

i) To collect and characterize the zircon sand from Tin Processing Plant in Jos. using a sodium iodide scintillation detector.

ii) To construct a source slab using zircon sand as source of radioactivity.

iii) To determine the distribution of radioactivity on the slab.

iv) To calculate theoretical doses at different distances from the centre of the slab.

v) To measure count rate using portable hand held GM tube and NaI(Tl) detectors.

vi) Determine calibration factor for some portable survey meters.

1.4 JUSTIFICATION OF THE RESEARCH

Point sources, which are used to calibrate radiation equipment in the lab, are not adequate in calibrating survey meters that are to be used in measuring environmental radiation. To be of use in defining radiation in the natural environment it is necessary that the measurement itself be consistent and has a direct correspondence to the terrestrial radiation. As such equipment used for such measurement has to be calibrated with calibration pad, which has been enriched with natural radioelement. Zircon sand that is a by-product of tin mining is in abundance and highly radioactive is being used as the source of natural radioelement in constructing the pad. Presently this is not available in the Centre for Energy Research and Training, Zaria. This

work will provide a prototype for future construction of such calibration pads. In so doing, it is hoped that this work will make great contribution in data collection from the environmental measuring facilities in the Centre. The data on radiation level in the natural environment also serve as a basis for comparison in the case of a nuclear accident. The air dose rate can be used as a basis for the calculation of the annual effective dose equivalent. Such measurements enable the recognition of areas of increased radiation and radon risks. This work is then a valuable contribution to standardization of measurements

1.5 THE SCOPE OF THE WORK

Calibration that is useful is energy specific. Therefore instead of using artificial radionuclides natural radionuclides in a matrix similar to what is available in the environment will be used to construct the calibration pad. The pad will then be used to test some of the radiation survey meters available at CERT. Since characterization of the zircon sand will be done in house, the quality of the result will depend on the equipment presently available in the Center. There will be a need to use internationally certified standards for constructing the calibration slabs in order to ascertain the quality of results obtained. This work may not go into details of this.

CHAPTER TWO

LITERATURE REVIEW

2.1 RADIATION

Radiation is energy in transit through space. It can consist of both waves and particles, which have many common characteristics. Mechanical radiation is made up of waves, such as sound waves, which require matter to be transmitted. Electromagnetic radiation on the other hand is independent of matter for its propagation, while matter affects its speed, amount and direction of energy. Electromagnetic radiation occurs in a variety of energies, with visible light about the middle of the range. Electromagnetic radiation with sufficient energy to bring about changes in the atoms it strikes is called ionizing radiation. Particle radiation can also be ionizing if it does not require matter for its propagation and has enough energy. Examples of particle radiation are cosmic rays, α-rays and β-rays.(Encarta,2002)

2.2 SOURCES OF NATURAL RADIATION

Natural radiation external to man includes terrestrial and cosmic radiation. Internal exposure results from radionuclei entering the body through ingestion and inhalation of naturally occurring substances in food, water and air. The natural radionuclides in the environment are of two general classes, cosmogenic and primordial. Cosmogenic radionuclides are produced through the interaction of cosmic rays with atoms in the atmosphere, and do not contribute significantly to external gamma radiation doses. Terrestrial component, being the major contributor to gamma radiation doses, arises from the primordial radionuclides potassium, uranium, thorium and their decay products (Nias 1990)

2.2.1 COSMIC RADIATION

Extra-terrestrial radiation is called cosmic radiation. There are two main sources of cosmic radiation. They are galactic and solar. Cosmic radiation reaches the earth from interstellar space and the sun. It is composed of a wide variety of penetrating radiations, which undergo many types of reactions with the elements they encounter in the atmosphere. Cosmic radiation is penetrating because it has high energy. The primary cosmic radiation that impinges on the earth's atmosphere consists of 87% protons, 11% alpha particles, and 1% electrons. Almost none of the primary cosmic radiation reaches sea level. The atmosphere acts as a shield that reduces the intensity of cosmic radiation, which reaches the earth's surface. This shielding action is the reason why the radiation level from cosmic radiation is less at sea level than at high altitude. The mean effective annual dose at sea level from cosmic radiation is about 0.25mSv, while the dose at altitude 3000m is about three times the dose at sea level. (Nias 1990).

2.2.2 TERRESTRIAL RADIATION

Terrestrial radiation is radiation from radionuclides that occur naturally from the earth's crust and in other materials from the earth. They are known as primordial radionuclides. They are long lived and have been present since the earth's origin.

Most radionuclides in nature are members of the three naturally occurring radioactive decay series. Each series consists of a sequence of radioactive transformations that begins with a long-lived radioactive parent and ends with a stable nuclide. In a closed environment such as the earth intermediate radioactive progeny exist in secular equilibrium with the parent. The decay of uranium and thorium to stable isotopes gives decay series comprising several tens of

radionuclides. Natural uranium is a mixture of the isotopes ^{235}U and ^{238}U with ^{235}U comprising 0.72% of natural uranium. (IAEA,1990) ^{232}Th is the parent element of the thorium decay series. Exposure to radon is the main contributor to radiation dose in many areas of the world. As a matter of fact the existence of gaseous radioactive isotopes of radon (short lived daughter radionuclides) in all the three naturally occurring decay series is responsible for presence of naturally occurring environmental radioactivity (Cember, 1992). The type of rock formation determines the concentration of naturally occurring radionuclides. The concentration is higher in limestone than in sandstone area. (Alan and Harbison, 1988).

2.2.3 RADIOACTIVITY IN THE BODY

The ingestion and inhalation of naturally occurring radionuclides give rise to a dose, which varies a lot depending on the location, diet and habit of the individual concerned. Potassium–40 and nuclides from the uranium and thorium series contribute most to this dose with minor contribution from carbon-14, which originates from the atmosphere. Naturally occurring potassium contains 0.0119% of isotope ^{40}K.that contributes about 0.2mSv per year to the population dose (IAEA-1990).

2.3 RADIOACTIVE DECAY

The nuclei of heavy elements found in nature are slightly unstable because they are large. For instance the isotope of uranium –238 having 92 protons and 146 neutrons may emit an alpha particle, in order to achieve greater stability. The nucleus becomes an isotope of Th with atomic number 90, and mass number 234. The decay process may be represented as $^{238}_{92}U \rightarrow ^{4}_{2}\alpha + ^{234}_{90}Th$. The effect of alpha emission in this instance is to produce a neutron rich nucleus that is still unstable. The nucleus tries to

attain greater stability by emitting a beta particle. The decay process is ${}_0^1 n \rightarrow {}_1^1 p + \beta^-$

All radioactive decays follow the same statistical law of radioactivity which states that in a sample of a particular radionuclide the number of atoms that disintegrate per unit time is directly proportional to the number of atoms present in the sample. This can be represented mathematically as dN/dt ∝- N which implies that dN/dt =-λN; where N is the number of atoms remaining and λ is the constant of probability known as the decay constant, which is actually characteristic of the radioisotope concerned. Activity, which describes the rate at which disintegration is occurring, is given as A = dN/dt, the unit of activity is the becqurel (Bq), one disintegration per second=1Bq (IAEA, 2003)

An earlier unit of activity is the curie (Ci) defined as $3.7 \times 10^{10} dps$, the original definition of the curie was based on the number of α particles emitted per second by radon in equilibrium with 1g of radium – 226. Even though the decay rate is now known to equal $3.61 \times 10^{10} dps$ the definition of the curie has remained as described. The becqurel and the curie are related by $1Bq = 2.7 \times 10^{-11} Ci$. The activity of a radioactive sample per unit mass is known as the specific activity of the sample. The relationship between the half-life and decay constant is $T_{½} = In2/\lambda = 0.693/\lambda$. The average lifetime or mean life of a radioactive sample is the average time required for the atoms of the sample to decay. This can be expressed mathematically as $T_{avg} = ⅓_{\lambda}$ (Hendee, 1996)

2.4 PHYSICAL INTERACTION OF RADIATION WITH MATTER

The electrical interaction as ionizing radiation transverses a medium is random. A small number of atoms in a medium are ionized or excited while most are unaffected

at low doses of radiation. While the energy transferred to the atom in excitation raises the energy level but does not change it, in ionization, electrons are removed from the atoms as radiation transverses the medium. Ionizing radiation consists primarily of high velocity charged particles like alpha particles and beta particles or secondarily when they are produced by indirectly ionizing radiation like gamma rays and neutrons. Photons eject electrons from atoms mainly by photoelectric effect, Compton effect and pair production. The energy of the photons and the properties of the medium through which they pass determine the process, which predominates. The linear energy transfer of the particle is the average energy deposited along the path of the particle per unit path length, and is dependent on the nature of the particle and its energy. (ICRP, 1990).

2.4.1 PHOTOELECTRIC INTERACTION

In photoelectric interaction total photon energy is transferred to an inner electron of the atom of the absorber. The kinetic energy of the electron ejected is given by $E_k = hv - E_b$ where hv is the incident photon energy and E_b the binding energy of the ejected electron, known as a photoelectron. Low energy photons eject photoelectrons at right angle to the direction of the incident photon. The ejected electrons create vacancies, which are filled by cascading electrons resulting in the emission of characteristic photons (X-ray) and auger electrons. Photoelectric effect is the most dominant type of interaction for low energy photons. The probability of photoelectric effect decreases with increasing energy. In general the mass attenuation coefficient for photoelectric absorption decreases as $(1/hv)^3$ whilst the cross-section for photoelectric absorption varies approximately as $z^4\lambda^3$ which is also given as $Z^5\lambda^{7/2}$. The probability for photoelectric effect increases as the z number of the

absorber medium increases. The energy of the photoelectron is lost in the absorbing medium mainly by excitation and ionization. The fluorescent radiation, which follows the initial interaction, is as a result of the binding energy being transferred to the absorber. Auger effect is the emission of low energy photoelectron after a vacancy is created in one of the inner atomic shells by photoelectric effect. The probability of auger emission and X radiation is measured by the fluorescent yield, which is given by

$$W_k = \frac{number}{number}\frac{of}{of}\frac{k}{shell}\frac{quanta}{vacancies} \text{ (for the K shell)} \qquad (2.1)$$

2.4.2 COMPTON EFFECT

In Compton effect, the incident gamma photon transfers part of its energy to an electron (which is regarded as free) in the absorber. This is possible if the initial momentum of the electron is less than the energy transferred to it by the incident photon. After the transfer of energy to the electron, the remainder appears as the energy of a scattered photon, with longer wavelength than the incident photon.

For Compton effect the energy and momentum will be given as follows; starting with conservation of momentum

$$\frac{hc}{\lambda} = \frac{h}{\lambda'}\cos\theta + p\cos\phi \qquad (2.2)$$

$$\text{and } 0 = \frac{h}{\lambda'}\sin\theta - p\sin\phi\,; \qquad (2.3)$$

where p is the momentum of the recoil electron and for conservation of energy

$$\frac{hc}{\lambda} + m_0c^2 = \frac{hc}{\lambda'} + mc^2\,, \qquad (2.4)$$

When ϕ and p are eliminated the change in frequency of the scattered photon

becomes

$$\frac{c}{v'} - \frac{c}{v_0} = \lambda' - \lambda_0 = \frac{h}{mc}(1 - \cos\theta) \qquad (2.5)$$

From the above, it is obvious that the Compton shift in wavelength $\lambda' - \lambda_0$ is, therefore independent of the incident wavelength and the material of the scatterer; it can be expressed in terms of the fundamental constants $\frac{h}{mc}$ (wavelength of a photon of energy equal to mc^2) and dependent on the angle θ. Compton effect occurs for gamma energies between 0.5MeV and 10MeV, which is the energy of most radioisotopes. The cross-section for this interaction decreases gradually with increasing photon energy; it is independent of the atomic number of the medium while the Compton mass attenuation coefficient increases with increase in electron density (electron per gram). (Karl and James, 1967).

2.4.3 PAIR PRODUCTION

This is an interaction of high-energy photons. As a matter of fact this process is only possible if the incident photon energy exceeds twice the rest mass energy of an electron (1.02MeV). As a result of this interaction an electron-positron pair is created, while the incident photon is annihilated. Any energy above 1.02MeV of the incident photon appears as kinetic energy of the electron-positron pair. The cross-section for pair production is proportional to Z^2. The total cross-section for pair production equals $\sigma_{pp} = \sigma_{pa} + \sigma_{ps}$, where $\sigma_{ps} = \sigma_{pp} . \frac{2mc^2}{hv_0}$ and σ_{pa} refers to pair absorption and σ_{ps} pair scattering, which refers to the disappearance of the positron and production of the annihilation quanta (Burhcam, 1963).

2.5 BIOLOGICAL EFFECTS OF RADIATION

Ionization changes atoms sometimes temporarily which lead to the molecules being changed. Excitation of atoms may also cause changes if the excitation energy exceeds binding energy between the atoms. The living cell containing the affected molecules may sometimes be damaged either directly if the molecule is critical to the cell's function or indirectly if adjacent molecules are chemically changed as happens in the production of free radicals.

DNA damage is the most serious damage radiation causes, because it may prevent the survival or production of the cell though the damage may be repaired in many cases. If the repair is not perfect it may lead to the proliferation of modified cell. If enough cells in an organ are killed or prevented from producing and functioning normally, the function of an organ may be impaired. This is known as deterministic effect. A modified somatic cell, which still retains its reproductive capacity, may give rise to a clone or modified cell, which may eventually lead to cancer. If the modified cell is a germ cell, it may transmit incorrect hereditary information to the descendants of the affected person resulting in abnormalities of the descendants. (ICRP, 1990).

2.6 RADIATION DETECTORS

High energy quanta and elementary particles are not directly perceptible by man in sub-lethal doses. As a result instruments of varying types have been devised to detect their presence and provide quantitative information relating to their energy, number and quality.

There are generally two types of detecting instruments; passive instrument that store up information as long as they are exposed to radiation and are usually inspected to

extract information (like in TLDs and photographic emulsions) and active instruments that produce an electrical signal indicative of the presence of radiation (like in Geiger counter). In all types of detecting instruments the nuclear radiation has to dissipate some of its energy within the sensitive volume. This energy which initially resides in the single primary particle is what then gets spread over the volume of the detector medium resulting in events on a macroscopic scale which enables an observation to be made. The energy dissipated in the medium results in ionization in some cases and a signal, which can be amplified and recorded. The interaction of the incident radiation with matter is by charged particles, because it occurs in the electronic structure. In the case of γ-rays and neutrons charged particles are first produced by the incident photon before they are detected. Ionization, secondary emission and fluorescence may thus be used in radiation detection. (Sharpe, 1955).

Detectors range in complexity from the well-known Geiger counter to room sized spark and bubble chamber. As scintillation and semiconductor detectors are going to be used in this work, their mode of operation will be fully discussed while other methods will be briefly mentioned.

2.6.1 GAS FILLED DETECTORS

There are three types of detector systems operated as gas-filled detectors; they are ionization chamber, proportional counter, and the Geiger-Muller tube. The variations of pulse size with increasing voltage across the electrodes determine the category of the gas filled detector.

DESCRIPTION OF THE SIX REGION CURVE

The graph below shows ions collected or pulse size on a logarithmic scale with increasing voltage applied on a linear scale. The curve is divided into six distinct regions, each having a name and distinct characteristics.

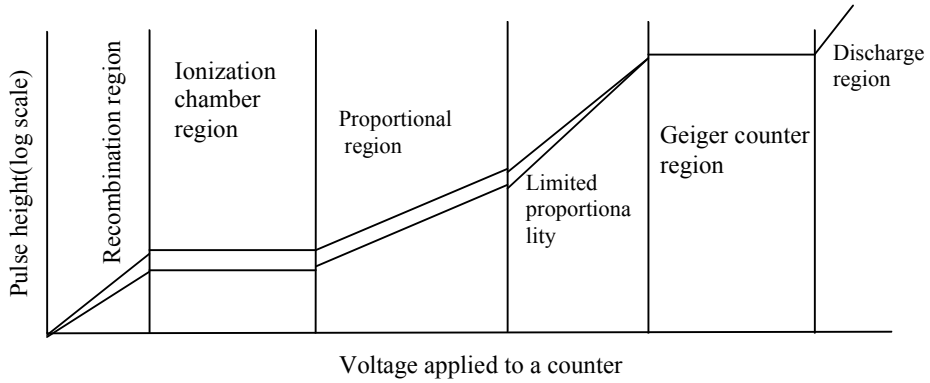

Fig. 2.1: Signal to Voltage Relationship for Ionization Chambers

Recombination Region: As the name suggests due to the low applied voltage the ion-pairs initially produced move slowly and hence recombine before reaching the electrodes. The ion-pairs collected are much less than what was initially produced; as such detectors are not operated in this region.

Ionization Chamber Region: Saturation occurs in this region as such pulse size does not change with increasing voltage and the curve is flat in this region. Every ion-pair produced is collected at the electrode. Ionization chambers are operated in this region.

Proportional Region: Gas amplification is said to occur in this region because the ion-pairs collected is more than that produced by the radiation. Gas amplification factor that is defined as the number of ion-pairs collected divided by the number of ion-pairs initially produced by radiation is a function of the detector type and the

applied voltage. As the amplification factor is the same at a specific voltage for any type of radiation proportional counters are operated in this region. Instruments operated in this region require a constant voltage supply and they usually are sensitive to low-level radiation.

Limited Proportionality Region: In this region the gas amplification factor is not the same at a specific voltage for any type of radiation; as such detectors are not operated in this region.

Geiger-Muller Region: In this region the output pulse is independent of the initial ionization event. Because of the avalanche produced by the electrons in the high electric field, the discharge is conveyed down the whole length of the anode. The electron that, are much lighter than the positive ion reach the anode much faster, while the slowly moving positive ions forms a sheath which acts as a partial electrostatic screen hence reducing the field at the anode below the value necessary for ionization. If a second pulse enters the detector during the avalanching period it will not be detected until the effect of the avalanche has been cleared. The time during which a second pulse could not be detected is called the dead time and it is approximately $10^{-6} s$. The time before a full size pulse can be produced is called the resolving time and it is approximately equal to $10^{-4} s$. The resolving time and the dead time are dependant on how fast the positive ion sheath gets to the cathode. A quenching gas (alcohol) with a lower ionization potential is added to the argon gas in order to neutralize the argon ion before reaching the cathode hence preventing the emission of ultraviolet light. It is thus the alcohol ions that reach the cathode and the energy available is used in dissociating the alcohol molecule.

Continuous discharge region: The very high voltage across the electrode leads to continuous electric arching across the electrodes, which results in a constant pulse that is not caused by the radiation entering the detector. For these reasons detectors are not operated in this region.

2.6.2 SCINTILLATION DETECTOR

A substance which absorbs energy and reemits it in visible or near visible radiation is said to be a luminescent material. The excitation and ionization by radiation, which leads to deexcitation from higher energy to lower or ground state energy level in such substances results in scintillation. Substances that emit light flashes when irradiated are referred to as scintillators. If the excited atom occupies an energy level above the undisturbed state, the deexcitation, which occurs in, $10^{-8} s$ is accompanied by light. The time dependence of the photon emission follows an exponential law, $N_p = K(1 - e^{-t/\tau})$ where k is a constant, N_p = number of light photon emitted in time t after the arrival of the ionizing radiation, τ = decay time or mean lifetime. In phosphorescence the excited state is metastable and the deexcitation is delayed. Impurities or activator may be added to the material to create more luminescence centers. The incident particle or photon leaves some electrons in excited states in scintillation counting. As they de excite to ground level they emit photons of UV or visible light in the form of light flash. The scintillation process must occur immediately the triggering occurs. The scintillator must be transparent to it's own scintillation. There are a wide variety of scintillation materials with divergent sizes and efficiencies. A scintillation counter comprises a scintillator an optical coupling system and a photomultiplier tube. The scintillator, which is the sensitive volume of the detector, generates the scintillation pulse, which is viewed by a highly sensitive

photomultiplier tube. The assembly of scintillator volume and PM-tube is enclosed in a light tight container to isolate the scintillation from ambient light otherwise the signal could be swamped and Pm-tube overwhelmed. The Pm-tube could be considered to be an electronic valve enclosed in an evacuated glass envelope. The tube usually has an end window of glass or silica depending on the type of light to be transmitted. The Pm-tube has a negatively charged photochatode and a series of intermediate electrodes, which are at successively higher potential called dynode, the photoelectrons which are produced in the photochathode are accelerated and focused on the first dynode because of the electric field. Secondary electrons are released for each incident electron. This process is repeated at each dynode resulting in the pulse being amplified as it travels through the tube. If the gain at each dynode stage is g and there are n stages, then the net gain is nxg. The Pm-tube could thus be considered to be a high gain pulse amplifier. As a matter of fact it is also a linear amplifier because if the P.D between dynodes is constant then the gain is constant so also net gain would be constant. Hence energy spectrometry is possible because there is a proportional relationship between the pulse height and the original signal deposited in the scintillator.(Adams and Dams, 1975).

There are five classes of scintillation materials, they are: organic crystals, liquid solution of organic materials, and solid solution of organic materials, inorganic crystals and noble gases. NaI (Tl) is the most common scintillator because of it's good light yield, excellent linearity and high atomic number of iodine and it's an example of extrinsic crystal because it is activated with thallium. It is usually sealed in an alluminium can with reflecting or diffusing walls because it is hygroscopic. The output of the scintillator is conveyed to the photosensitive cathode surface of a sealed off photomultiplier tube. The input at the photosensitive cathode is multiplied

several thousand times by the application of positive voltage between successive dynodes in the photomultiplier tube. As a matter of fact a gain of $10^7 - 10^8$ is achieved by the time the electrons reach the last dynode stage that is called the anode, from where an electrical pulse is taken out for further analysis.

High ionization density impedes energy transfer in organic phosphor; it affects inorganic phosphors to a lesser extent while gaseous scintillators are not affected at all. The time taken by the electrons to reach the anode (transit time) and the stability of the electron multiplication factor determine the quality of the photomultiplier tube. It has been found that: $V = Q/C$ where V is the output pulse height, C is the capacitance at the output and Q is the charge collected at the output. It can be shown that the output charge collected Q equals; $Q = N_e e = eMf_d f_m f_p \varepsilon_i f_n E_n$, where E_n is the energy of the incident radiation, f_n is the fraction of this energy dissipated in the scintillator, the scintillator converts the energy $f_n E_n$ into light with an efficiency ε_i, $f_p \varepsilon_i f_n E_n$ is the amount of light energy which reaches the photocathode, where f_p is the fraction of the photons which reach the photocathode, f_m is the number of photoelectrons emitted by the photocathode and f_d the fraction of the photoelectron collected by the dynode and M the multiplication factor. (Singru, 1972).

The response function of a sodium iodide (thallium activated) gamma ray detector depends on the size, shape, and composition of the detector and the geometric details of the irradiation conditions.

2.6.3 SEMI CONDUCTOR RADIATION DETECTORS

A semi conductor is a material, which has electrical properties between an insulator and a conductor. The lattice of crystalline material exists in allowed electron energy

levels, which are packed into bands that are separated by an energy gap known as forbidden gap ($E_g \approx 1eV$ for semi conductor). An electron in the pure semi conductor material is confined to a specific band. The lower electron energy level, known as the valence band is completely filled by valence electrons that are bound to specific lattice sites while the higher electron energy level known, as the conduction band is completely empty at 0°K. Electrons in this band are free to move within the crystal and contribute to the electrical conductivity of the material. At higher temperatures an electron in the valence band might get excited and obtain sufficient energy and jump the forbidden gap to the conduction band. The excitation of an electron or net negative charge into the conduction band leaves a hole or net positive charge in the valence band. The probability of generating an electron-hole pair is a function of temperature given by the expression:

$$p(T) = CT^{3/2} \exp\left(-\frac{E_g}{2kT}\right) \qquad (2.6)$$

where T = absolute temperature in Kelvin, E_g = band gap energy k = boltzmann constant and C = proportionality constant characteristic of the material

The electron-hole pair constitutes the charge carriers as they contribute to the overall conductivity of the material. The drift velocity or net migration of electron-hole pair at the application of an electric field is proportional to the applied electric field until saturation is reached. The ionization energy, which is the amount of energy required to create the electron-hole pair, is about 3eV that is $1/10^{th}$ of the energy required to create an electron-positron pair in gases. Since there are more charge-carriers created in semiconductor than in gases for equal incident photon energy, the statistical fluctuation becomes smaller.

Some of the advantages of semi conductor detectors over gas-filled or scintillation detectors are that they are smaller, faster rise time of the output pulse, better linear response over a wide range of energy, excellent energy resolution and choice of sensitive depth, area and configuration. For semi conductor detectors the pure crystal (mostly silicon and germanium, both group four elements) is doped with an impurity. If the impurity is a pentavalent element like phosphorus, four of the electrons will be used in forming the covalent bonds while the extra electron will occupy a position in the forbidden gap just below the conduction band hence it will require very little energy to raise it to the conduction band. Such types of impurities are referred to as donor or n-type impurities because of the ease with which an electron is released to the conduction band and thus contribute to the general flow of current. The total charge carrier in doped material is much higher than in the pure material, hence the electrical conductivity is much higher. Electrons are majority carriers while holes are the minority carriers. If on the other hand a trivalent element like boron is the impurity, it will result in one valence bond unsaturated and an acceptor level in the forbidden gap very close to the valence band is created. Thermally excited electrons easily fill such acceptor sites. In this case the impurity is called acceptor or p-type because it accepts electron and holes are the majority carriers. The mobility of charge carriers is adversely affected by trapping and recombination. In trapping the charge carriers get trapped in the impurity centers and it usually takes sometime for such trapped electron or hole to get back to the normal band hence leading to a reduction of charge carriers. In recombination the electron and hole recombine, hence also reducing the number of charge carriers. A single crystal is used for the p-n junction. If we start with a p-type crystal one surface of the crystal is exposed to the vapour of an n-type impurity; such vapour will diffuse into the crystal and once

the donors outnumber the acceptors on such a surface an n-type region is formed. The junction between these two regions constitutes a discontinuity in the conduction of electron density; there will therefore be diffusion from regions of high concentration to that of lower concentration. When an external electric field is applied, electrons from the n-type region will flow to the positive electrode while holes will be swept to the negative electrode, and this movement of charge carriers to opposite poles result in the region between the n-type and p-type regions being cleared of charge carriers of both signs. This region is known as the depletion layer. If an ionizing radiation passes through the depletion layer electron-hole pair will be created which will flow to the electrode and as such produce a pulse to signal the passage of radiation. The major setback of this type of detector is the fact that the ionizing radiation has to pass through a thick region of n-type or p-type material before getting to the depletion region. (Knoll, 1989).

LITHIUM DRIFTED GERMANIUM DETECTORS

Germanium is more suited than Silicon for detecting gamma rays because of its higher atomic number. Ge (Li) is prepared by zone refining to get a high quality p-type germanium of cylindrical shape. Zone refining entails heating the material and slowly passing the molten zone from one end of the sample to the other as a result the impurities are transferred to the melted zone and hence can be swept from the sample. Lithium ions are diffused into the germanium by applying high electric field, until an n-type region is formed. The drifted lithium ions neutralize the p-type impurities in germanium and hence give rise to a region of intrinsic material. The intrinsic region which is usually devoid of charges of both signs forms the active volume of the detector where ionizing radiation create electron-hole pair that are collected by external electric field. This detector has to be maintained at 77K by

mounting the crystal in a vacuum cryostat thermally connected to a copper rod in order to prevent thermally induced leakage current, which take place at room temperature. (Singru, 1972)

HIGH-PURITY GERMANIUM DETECTOR

Zone refining is used to process bulk germanium. In this process the impurity level is progressively reduced by heating the metal and slowly passing the molten zone from one end of the sample to the other, which leads to the impurities being transferred to the molten zone and removed from the sample. Impurity levels as low as $10^{10}\, atoms/cm^3$ are obtained for the high purity germanium crystals grown from this purified stock. If the remaining impurities are acceptors, the semi conductor crystal becomes mildly p-type whilst if the impurities are donors then high purity n-type result. The main advantage of HpGe is that they can be warmed to room temperature between uses without any detrimental effect while Ge(Li) detectors have to be continuously maintained at liquid nitrogen temperature. As already mentioned the characteristics used in selecting a semi conductor detector are, energy resolution and peak shape, peak to Compton ratio efficiency, crystal or well dimension, and price

Energy Resolution and Peak Shape:

The ability of a detector to separate closely spaced peaks is known as energy resolution and it also assists in detection of weak sources when superimposed on a broad continuum. Energy resolution is a function of statistical spread in the number of charge carriers created, charge collection efficiency and electronic noise. The full width at half maximum of a typical full energy peak or photopeak is given by:

$W_T^{\,2} = W_D^{\,2} + W_X^{\,2} + W_E^{\,2}$ where the W values on the right hand side are the peak widths that would be observed due only to the charge carrier statistics, collection of

charge carriers and electronic noise. The variation of charge carriers created is given by $W_D^{\,2} = 2.35^2 F\varepsilon E$ where F is the fano factor, ε the energy required to create one electron-hole pair, while E is the gamma ray energy. The efficiency of charge carrier collection is dependent on the detector active volume and electric field strength. The peak shape of germanium detector can be estimated using gaussian distribution even though there is tailing off at low energies due to imperfect charge collection in some region of the detector or secondary electron or bremsstrahlung escape from the active volume. The full width at one tenth maximum should be less than double the full width at half maximum for good quality detectors with minimum tailing. The ratio of $FW.IM/FWHM = 1.823$ for pure gaussian peak, (Knoll, 1989)

Peak to Compton ratio: This is an index of performance of the semi conductor detector. It is defined as the ratio of the count in the highest photopeak channel to the count in a typical channel of the Compton continuum associated with that peak. It can also be defined as the ability of the detector to distinguish low energy peaks in the presence of high-energy sources. This ratio is a function of the detector energy resolution and photofraction and structural materials near the detector or source also affect this ratio. (IAEA, 1990)

Due to the fact that gamma rays have to undergo interaction within the active volume of the detector before detection of radiation is possible, the efficiency is less than 100%. There are two categories of counting efficiencies; they are absolute efficiency and intrinsic efficiency.

$$\text{Absolute efficiency} = \frac{No\ of\ pulse\ recorded}{No\ of\ quanta\ emitted\ by\ source}, \text{ while}$$

$$\text{Intrinsic efficiency} = \frac{No\ of\ pulse\ recorded}{No\ of\ quanta\ incident\ on\ \text{detector}}$$

While the intrinsic efficiency depends only on the detector properties, the absolute efficiency on the other hand depends on both detector properties and counting geometry. The absolute radioactivity of a source can be measured once the efficiency of the detector to be used is known.

$$S = N\frac{4\pi}{\varepsilon_{ip}\Omega} \tag{2.7}$$

ε_{ip} = Intrinsic peak efficiency

N= No of events under the full energy peak in the detector spectrum.

S = radiation quanta emitted by the source.

Ω = Solid angle subtended by the detector at the source position.

$$\Omega = \int_A \frac{\cos\alpha}{r^2} dA \tag{2.8}$$

where r is the distance between the source and a surface element dA, and α = the angle between the normal to the surface element and source direction. The solid angle Ω for a point source located along the axis of a cylindrical detector is given as:

$$\Omega = 2\pi\left(1 - \frac{d}{\sqrt{a^2 + d^2}}\right) \text{(Tsoulfanidis,1983)} \tag{2.9}$$

where d is the source to detector distance and a is the detector radius.

Crystal or Well dimension: Ge(Li) detector configuration can be either coaxial or planar. The planar configuration detectors are usually small with low capacitance and low noise level and they give very high resolution. They are suitable for the detection of low energy photons. Larger active volumes can be obtained with coaxial configuration as such they are more common and hence they can be used in detecting high-energy gamma rays. As a matter of fact while the total active volume for planar

configuration cannot exceed $10-30cm^3$ the coaxial configuration can reach $400cm^3$. Detectors whose crystal dimensions exceed their length are best suited for measurement of gamma energies less than 1 MeV. (Knoll, 1989) From the inverse square law the closer the distance of the source to the crystal the better the sensitivity of the detector but due to the fact that geometric errors increase with closeness of the source to the crystal, there is a limitation of how close the source is to be placed to the crystal. Detectors with hole through have higher resolution than blind-hole type, which on the other hand has better efficiency because of the active material at the bottom. (IAEA, 1990)

2.6 CALIBRATION OF DETECTION EQUIPMENT

Calibration can be defined as the quantitative determination, under a controlled set of standard conditions, of the indication given by a radiation-measuring instrument as a function of the value of the quantity the instrument is intended to measure. An equipment is calibrated for the under listed reasons:

i) To ensure that an equipment is working properly.
ii) In order to ascertain the error of the equipment reading or readjust the equipment for those provided with calibration adjustments.
iii) To determine the relation between a devise reading and a really measured quantity.
iv) In order to place confidence limits upon measurements made with equipment.
v) To provide consistent radiometric measurements.

A radiometric equipment can be calibrated for energy and efficiency as follows:

Energy Calibration: Gamma ray spectrometer whether NaI(Tl) scintillation detector or semi conductor detector used to measure energy distribution curve can be calibrated for energy. As the main features of such distribution curves are peak positions; the data acquired can be used to identify the energy of the gamma

radiation. This is carried out with curves of channel-energy relationship. Sources of known radionuclide content have gamma energies in the range of interest with at least two samples. Those that are sufficiently separated and are easily measurable are selected. Data is acquired for sufficient time required to get adequate counts of the peak of interest. The position of the peak is determined with an accuracy of a tenth of a channel. The expression for peak position is given by;

$$P = \frac{\sum_{i=a}^{b} iN_i}{\sum_{i=a}^{b} N_i} \qquad (2.10)$$

where N_i is the number of counts in channel i and a and b are the lower and upper limits of the channel. A straight-line graph of peak positions against energy obtained from nuclide table is plotted.

Efficiency Calibration: Factors, which affect the efficiency calibration and have to be taken into consideration are; sample counting geometry, calibration method, calibration sources and analytical efficiency expression.

Sample Counting Configuration: Several containers with practical geometries are selected taking sample matrices into consideration. The dimension of the container should be well suited to the dimensions of the detector.

Calibration Method: Calibration standards are prepared for each counting configuration from calibration source whose density and matrix should almost be identical to the actual sample to be analyzed.

Calibration Sources: Certificate supplied with radionuclide selected for use as standard in efficiency calibration should contain the following; uncertainty associated with the activity, reference date, purity, mass or volume, chemical composition, values of half-lives, emission probability for all modes of decay.

Calibration points should adequately cover the energy range to ensure that interpolations within the range are accurate.

Table 2.1 List Radionuclides Often Used For Efficiency Calibration (1AEA,1998)

Radionuclide	Half-Life	E (keV)	Emission probability p_γ
^{22}Na	950.4d	511.00 1274.54	1.807 0.9994
^{46}Sc	83.80d	889.28 1120.55	0.99984 0.99987
^{51}Cr	27.71d	320.08	0.0985
^{54}Mn	312.5d	834.84	0.99975
^{57}Co	271.84d	122.06 136.47	0.8559 0.1058
^{60}Co	1925.5d	1173.24 1332.50	0.9990 0.999824
^{109}Cd	436d	83.03	0.0368
^{137}Cs	30.0a	661.66	0.850
^{139}Ce	137.65d	165.853	0.800
^{141}Ce	32.50d	145.44	0.489
^{203}Hg	46.612d	279.20	0.813
^{241}Am	420.0a	59.54	0.360

Analytical Efficiency Expression: After data is acquired the expression shown below is used for determining the efficiencies of gamma energies from 200keV to 3000keV.

$$In\varepsilon = a_1 + a_2 InE \qquad (2.11)$$

where Inε is the natural log of the absolute full energy photopeak

$a_1, a_2 =$ fit parameters

E =the energy (keV) of the corresponding gamma line.

Spectrometer efficiency can also be calculated using the expression shown below:

$$\varepsilon = \frac{\left(N - N_b\right)}{tAP_\gamma} e^{\frac{0.693\Delta t}{T_{1/2}}} \qquad (2.12)$$

where N =counts in the peak at energy E

N_b = Background counts in the peak energy E

t =measurement live time (s)

A = activity of the prepared standard at the reference time stated in the certificate.

p_γ = Emission probability for gamma ray with energy E

Δt = time elapse since the reference time which is usually stated in the certificate

$T_{½}$ = Half-life of the radionuclide

Efficiency can be plotted against energy on a log-log diagram (IAEA, 1998)

2.8 SECULAR EQUILIBRIUM

In the natural radioactive series the nuclides in the series decay to their immediate daughter at a rate that is dependent on the half-life of the nuclide concerned. A decay series is said to be in equilibrium when the rate at which a nuclide is produced by decay is equal to the rate at which it decays for each of the nuclide in the series. This in effect means the activity ratio between any two nuclides in the series in unity as such satisfy the condition $N_1\lambda_1 = N_2\lambda_2 = N_3\lambda_3 .... = N_n\lambda_n$ where $N_1, N_2, ...N_n$ is the number of atoms in the nuclide 1,2…n and $\lambda_1, \lambda_2, ...\lambda_n$ are their respective decay constants. The nuclides with short half-life will reach equilibrium first so that by the time the longest lived daughter reach equilibrium, the whole series would have reached equilibrium. This in effect means that the whole series will reach equilibrium when the longest lived daughter reaches equilibrium.(Dewu,1993).

2.9 REVIEW OF PREVIOUS WORK

Ajayi, *et al*. have used NaI(Tl) to measure radiation from environmental samples in their work on the natural radioactivity in Ijero-Ekiti, they sealed their samples for 4weeks to allow enough time for the radionuclides to reach secular equilibrium. The activity of ^{214}Bi was taken to represent ^{238}U while that of ^{298}Tl was used to represent

the activity of ^{232}Th. NaI(Tl) was used to acquire counting data. It was discovered that the mean absorbed dose due to ^{40}K, ^{238}U and ^{232}Th was 35.19nG/h, which is equivalent to 0.35Sv/yr. This value is much lower than the maximum permissible dose to the public. The area is therefore free from any radiological contamination. (Ajayi,. *et al.*, 1995).

In a similar work carried out by Ajayi, *et al (1996)* in a part of southwestern Nigeria, it was discovered that the absorbed dose in both the rainy and dry seasons was 20.47nGy/hr, that is equivalent to 0.18mSv/yr. This is therefore below the ICRP recommended permissible dose to the public.(Ajayi, *et al.*, 1996)

Ibeanu's (1999) work in the tin mining area has shown that the trend in activity concentration is Th> Ra> K instead of the normal average environmental activity of K> Th>Ra. This trend has been attributed to the high thorium content of monazite and zircon that are both tin associates. The high concentration of the Th content is attributed to the insoluble and immobile nature of thorium that makes leaching and transportation of thorium less compared to that of uranium. In-situ measurements of the site used for Ibeanu's (1999) work was with NaI(Tl) detector (Ludlum model 44-2) that was calibrated with Cs-137 point source.

From Rabi'u (1993) it has been determined that the gross activity of soil, plant and water ranges from about 0.1-2.5Bq/g, 0.3-6.0Bq/g and 0.1-0.3cps respectively for Jos tin worked area. Zircon and monazite have the highest activities of 77Bq/g and 96Bq/g and highest dose rates of 370mSv/yr and 790mSv/yr, which are obviously above the maximum permissible, dose to the general public of 1mSv/yr. The area is therefore not suitable for habitation. From the Th and U concentrations and the Th/U ratio it maybe said that the major source of radioactivity is the thorium and the

radioactive mineral are mainly monazite and zircon. In each case Rabi'u (1993) measured three U and Th standard and the calibration curves plotted for the respective peaks.

The activity of soil is greatly affected by the activity of dumped tailings, which means that tin mining and processing activities has led to technologically enhanced naturally occurring radioactive materials (TENORM) in the Kuru environment. Ibeanu (1999). The statistical analysis of the measured and computed dose rates of samples from Kuru and control (being an example of normal soil) indicate the following from Ibeanu's work.

i) The measured and computed data for the control area are close to normal, which is as a result of the homogenous nature of the soil. There is record of TENORM and this is confirmed by the result.

ii) The dose rate values for the control both measured and computed show that the mean, median and modal values are almost identical which is an indication of a symmetrical distribution.

iii) The Kuru measured dose rates were obviously influenced by the activity of the dumped tailings, which effectively cancelled out the effect of soil activity concentration. The dose rate distribution of the Kuru data was found to be asymmetric with a skew to the right, because of the great variability of the data. The distribution of the recorded dose rate showed that 60% are less than 8.0μG/hr about 25% are less than 12.0μG/hr the remaining 15% were extreme values hence they tailed off. Each dose rate represented the effect of the tailing concentrations dumped at the particular spot as a result there is no agreement between the measured and the computed dose rates. The difference

in the mean, median and modal values of the Kuru computed dose rate is an indication of the asymmetric and lognormal nature of the distribution. The difference in trend of activity concentration levels between normal environment (K> Th> Ra) and tin worked environment (Th>Ra>K) is confirmed by Ibeanu (1999).

2.10 CALIBRATION PAD

A calibration pad is a slab of concrete containing known concentrations of radioelements. Ideally calibration pads should simulate geological source of radiation. The IAEA (1989) recommends four cylindrical concrete pads of 3m diameter and thickness 0.5m for calibrating large detectors, while smaller pads of (1x1x0.3m) are suitable for calibrating portable detectors. Each of the pads is enriched with either K, U or Th while the fourth pad serves as background for control, Grasty, et al (1991). Potassium, Uranium and Thorium and their decay products are the most significant sources of terrestrial radiation because they are the only natural radioisotopes, which produce gamma rays of sufficient energy and intensity to be measured by gamma ray spectrometry. Hence the reason why they are used as the radioelements for constructing calibration pads.

The recommended concentrations of the radioelements are 8% K in K-pad, 50ppm U in the U-pad and 125ppm Th in the Th-pad. Instrument sensitivities is derived from the calibration experiments. Since the detector response is evaluated against the concrete pads with known concentrations of radioisotopes, the detector response in counts per second can therefore be converted to concentration in pCi/g. (IAEA, 2003).

2.11 ZIRCON

Zircon is a transparent mineral, which is translucent, or opaque. It's main constituent is Zirconium silicate, $ZrSiO_4$. Its crystal has a tetragonal shape with a specific gravity of 4.2 to 4.86 and hardness of 7.5. Zircon shines with a luster like diamond and may occur as colourless crystal or in shades of green, grey, red, blue, yellow, or brown. The transparent yellow, orange, red and brown types called hyacinth or jacinth are used as gemstones. The very useful property of zircon is that it contains uranium and thorium, which are radioactive even though it is chemically and physically stable. The uranium lead ratio can be used for dating. (Encarta, 2002) Zircon occurs as an accessory mineral in all types of igneous rock and is abundant in silica rich rocks. In Jos Plateau zircon is recovered as a by-product of tin mining. (Rabi'u, 1993)

2.12 ANALYSIS

The self-absorption of the source material and the paths taken by photons from different parts of the source need to be accounted for in the calculation for source strength at a given point. The primary uncollided flux from the volume source is obtained by integrating the point kernal over the dimension of the source for a point source located a distance r in air from the point of measurement, the photon flux density is given by: $\Phi = \frac{BSe^{-\mu r}}{4\pi r^2}$ (2.13)

Where S is the source strength in photons per second, μ is the linear attenuation of air for the energy photons from S, B the buildup factor. The buildup factor is used to account for the scattering from the different photons for each region of the source by integration. The radioactive source is distributed uniformly and isotropically in the slab of thickness L, which is mixed with concrete of attenuation coefficient μ_s. The

differential detector response at position P from a segment of the slab dx is given by

$$dR(P) = 2\pi\Gamma S_v E_1(kt + k_s x)dx \qquad (2.14)$$

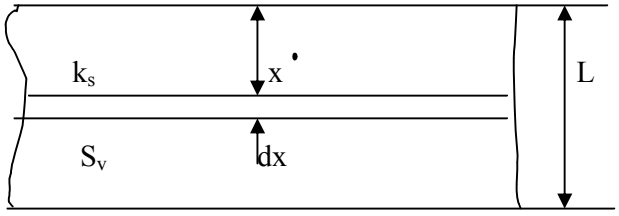

Figure 2.2 Differential Section through Source Slab

The total detector response is

$$R(P) = 2\pi\Gamma S_v \int_0^L E_1(kt + k_s x)dx \qquad (2.15)$$

If a change of variable is made, such that y = kt +k_sx then

$$R(P) = \frac{2\pi\Gamma S_v}{k_s} \int_{kt}^{kt+k_s L} E_1(y)dy \qquad (2.16)$$

Exponential integral function have the property that

$$E_n(y) = -\frac{d}{dy}E_{n+1}(y) \qquad (2.17)$$

Hence $$R(P) = \frac{2\pi\Gamma S_v}{k_1}[E_2(kt) - E_2(kt + k_1 L] \qquad (2.18)$$

If the slab is unshielded like it is in this case then the detector response becomes

$$R(P) = 2\pi S_v \Gamma \frac{e^{-\mu L}}{\mu} \qquad (2.19)$$ (Karl and James,1967)

Where Γ = specific gamma constant, which is defined as the exposure rate from a point source of a strength of 1Ci measured at a distance of 1m in vacuum. It is given according to (Khan, 1992): as equal to

$$\Gamma = \frac{3.7\times10^{10}\times3600(h^{-1})}{4\pi(m^2)}\frac{1(R)}{.00876(J/kg)}.1.602\times10^{-13}(\frac{J}{MeV})\sum_{i=1}^{N} f_i E_i(MeV)\left(\frac{\mu_{en}}{\rho}\right)_{air,i}\left(\frac{m^2}{kg}\right) \quad (2.20)$$

$$=193.8\sum_{i=1}^{N} f_i E_i\left(\frac{\mu_{en}}{\rho}\right)_{air,i}\left(Rh^{-1}\right) \quad (2.21).$$

where f_i is the number of photons emitted per decay of energy E_i

$\left(\frac{\mu_{en}}{\rho}\right)_{air,i}$ is the mass energy absorption coefficient in air for photon of energy E_i

S_v is defined as the activity per unit volume of the volume source.

$\frac{1}{k} = \frac{e^{-\mu L}}{\mu}$ which is the result of the exponential integral function to take care of the photons at the bottom of the slab.

Hence R(P) = $\frac{2\pi S_v}{r^2}193.8\sum \frac{f_i E_i (\mu/\rho)_{air,i} e^{-\mu l}}{\mu}$ (2.22)

CHAPTER THREE

MATERIALS AND METHOD

3.1 INTRODUCTION

This chapter discusses the materials and the method used in carrying out this investigation. Zircon sand was collected from N'gell Valley Tin Mining Company. Zircon sand cement and water were mixed in appropriate proportions to construct the calibration slab. The zircon sand was characterized with NaI (Tl) detector. The NaI(Tl) detector was calibrated for efficiency using certified standard point sources. Measurement of radioactivity was taken at different distances and angles with NaI(Tl) and GM-tube detectors over the slab constructed.

3.2 COLLECTION OF SAMPLES

Burham cement was purchased from a retailer in Tudun Wada Zaria. The zircon sand was collected from N'gell Valley Tin Mining Company, located at 42km along Barikin Ladi road in Plateau State. The zircon sand is a by-product of refining tin and columbite. It could be considered to be a tailing that is not thrown away in the dump. It is kept and given out on request.

3.3 SAMPLE PREPARATION

3.3.1 ZIRCON SAND

Zircon sand was homogenized by grinding it for 5minutes with Fritsch Puluerisette type: 02:102 No 4197 grinding machine. The grinding and crushing of sample is to ensure the sample was homogenous and also to provide identical counting geometry for reproducibility of result (Ibeanu, 1999). Empty plastic container of 6.5cm x 6.5cm was weighed and the plastic container was then filled with zircon sand and then reweighed. The lid of the plastic container was sealed with scotch masking tape.

The sealing was to ensure gaseous components of the uranium and thorium series are trapped. The sample was then left over a month to attain equilibrium.

3.3.2 CEMENT

Cement was not grinded because the size of the grain of the cement used 5.5μm according to the table on cement fineness (Agbazue, 1992), was considered to be quite suitable for this work. The empty plastic container was weighed, filled with cement and then reweighed again. The lid of the container was sealed with masking tape. It was then allowed to attain equilibrium.

3.4 STANDARD

A mixed IAEA standard of RGU-1, RGTh-1 and RGK-1 weighing 11.9g each with a net weight of 35.9g sealed 28th march 2001 of known concentrations was counted for 21600s. The net count was noted. The activity of ^{232}Th or any of its daughter states was representative of the activity of the parent. The activity concentration of ^{208}Tl was considered to be indicative of thorium and it occurred at 2614keV. The activity of ^{214}Bi at the gamma energy peak of 1763kev was taken to be representative of the activity of uranium. The energy peak occurred at 1460keV.

3.5 SCINTILLATION DETECTOR

NaI (Tl) detector Canberra model 802-4 serial no 8904425 with 7.62x7.62 crystal was used for the counting. The photomultiplier tube was also Canberra model 2007P. The detector and PMT tube were housed in a 2cm copper lining, 1mm Cadmium and 6cm lead, to shield the samples being counted. The detector was connected to a HV supply ORTEC 456 while the PMT was connected to amplifier ORTEC 485 positive bias and bipolar. The amplifier was connected to the computer interface or MCA Simulator. The software installed in the computer was Maestro for windows Model

A65-B1 version 3.20 and it provided advanced multichannel analyzer capabilities. The amplifier coarse gain was set at 2 and fine gain was set at 4. The maestro software gives the net count. The net count divided by the time spent in counting and the weight of the sample gave the specific activity of the sample. Comparing the activity of the standard and its concentration with that of the sample would give the concentration of the sample.

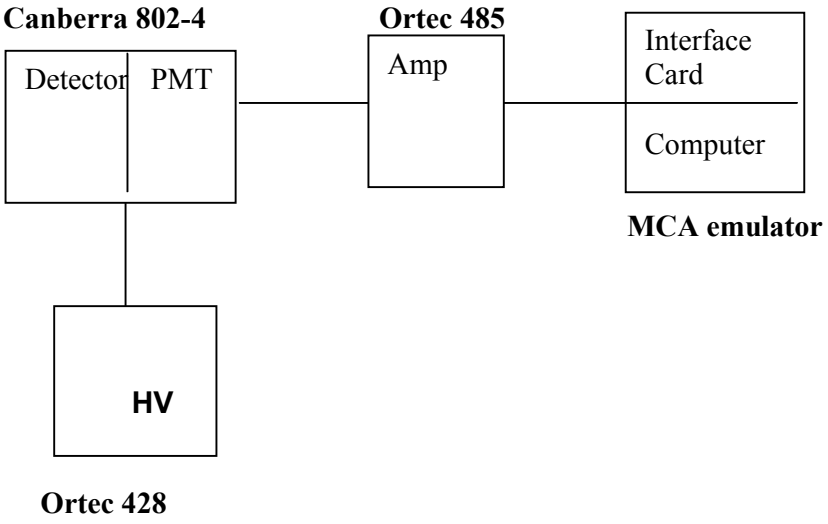

Fig.3.1 Block diagram of the NaI(Tl) Spectrometer

3.5.1 CALIBRATION

The detector was calibrated using ^{137}Cs and ^{60}Co to assign channel number to photon energy. The ^{137}Cs 661.6keV was set at 444 while that of ^{60}Co 1332keV was set at 900. The calibration for energy made it possible to relate energy to channel number.

3.5.2 COUNTING

Mixed IAEA standard of KUTh was counted for six hours (21600s). The potassium ^{40}K energy line was identified at about 1459keV, for ^{238}U, the ^{214}Bi at 1763keV was identified while ^{208}Tl at 2614keV was identified to be representative of the thorium series. The sample of zircon and cement were each counted for six hours (21600s) because the ^{214}Bi energy line was not discernable when the sample was counted for three hours. The specific activities of the standards were calculated while those of the samples were also calculated by comparing the net count area of the standard and that of the sample.

3.6 CONTRUCTION OF CALIBRATION PAD

For cement to hydrate, it requires a certain amount of water theoretically at least 0.4g to 1g of cement according to Portland Cement Association, (1975), but Abdulrashid, (2000) had experimentally found out that the best ratio of water to cement for optimal quality was 0.35g of water to 1g of cement. In order for cement hydration to continue the water must be allowed to evaporate. For this reason it might sometimes be required to provide curing which supplies additional water or inhibits initial water loss. The calibration slab was essentially a mortar slab. Mortar is a mixture of cement, sand and water in appropriate proportions (one part cement to two parts sand or 1part cement to three parts sand). When sand was mixed with cement in the proportion of 3 to 1 not more than 9 to 12.5% by weight of water would be required) (Kidder Parker- 1968). A 10ml mixture in the above proportions was tested; it was found that the water was inadequate. The ratio of 1part cement to 2 part zircon sand was therefore used. The density of cement and zircon sand were first determined. The weight of known volumes of each sample was determined; the mass was then

divided by the volume to obtain the density. The mass of the samples (zircon and cement) was determined by multiplying the appropriate volume with the density. The required masses of zircon sand and cement were measured and zircon sand and cement were thoroughly mixed with a shovel and trowel. The required volume of water was then gradually added while the mixture was being mixed. After mixing, the mixture was poured into the 1m by 1m open square base wooden box and mixture leveled with a trowel.

EXPERIMENTAL STAND

Fig. 3.2 shows the zircon cement calibration pad with the stand spread out and the X-ray gamma radiation portable detector in place. The stand is used only at the center of the slab. In all the other positions where measurements were taken, the detectors used were hand held.

Fig. 3.2 Experimental Stand

Figure3.2: Calibration Pad with Stand and Portable detect

MEASUREMENT POSITIONS

The figure 3.3 shows a representation of how the pad was partitioned into grids of 0.25x0.25m, to facilitate measurement at the center of each square. As a result measurements were taken at seventeen points.

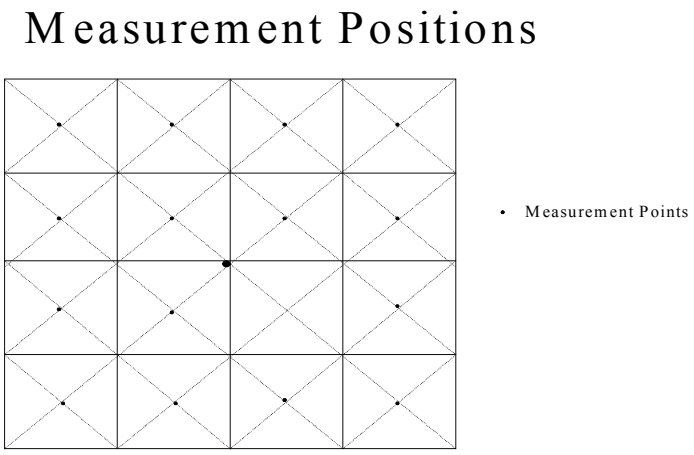

Figure3.3:Calibration pad partitioned into grids

Partitioning into grids enabled measurements at equidistant positions. NaI(Tl)(LUDLUM, M3) and GM-Tube(LUDLUM, M3) survey meters were used to take measurements at the center of each grid, at different heights. Plastic scintillator(ATOMTEX) and Energy compensated GM-Tubes(RADOS) detectors were used to take readings at the center of the pad at different heights.

3.7 RADIATION LEVEL MEASUREMENT

Measurement of radiation intensity were taken over the calibration slab at 5cm, 25cm, 50cm, 75cm and 100cm with the NaI(Tl) (Ludlum M3 survey meter) and GM tube (Ludlum M3) detectors at the center of each grid. These two detectors are portable hand held and are usually used for field measurements. Plastic Scintillator detector (Atomtex AT1121) and Energy compensated GM-Tubes (RADOS RDS-

120) detector are both hand held survey meters that, were also used to take measurement of dose rate above the center of the pad at different distances from the pad.

3.8 DETECTORS

3.8.1 LUDLUM MODEL 3 SURVEY METER

There were two LUDLUM M3 Portable survey meters used. One is a NaI(Tl) scintillation detector while the other is a GM-Tube. The operating range of the GM-tube is 0-500kCPM(counts per minute), while the Scintillation has an overall range of 0-200mR/h. The range is achieved by the use of four linear range multipliers of x0.1,x1,x10, and x100 in combination with 0-2mR/h meter dial for NaI(Tl) and 0-5kCPM meter dial for GM-tube. The normal operating voltage is set at 900V, even though it can be externally be adjusted to between 400 and 1500V for special requirement. Its response for 90% of final reading is from four to twenty two seconds.

3.8.2 X-RAY AND GAMMA RADIATION PORTABLE DOSIMETER

X-Ray and Gamma radiation portable dosimeter AT1121 otherwise known by its trade name of ATOMTEX is a portable dosimeter, which uses a plastic scintillator with photomultiplier as detector. It can measure continuous X-ray and gamma ambient dose rate equivalent radiation and dose rate equivalent during short-term radiation influence. Its range for continuous measurement is from 50nSv/h-10Sv/h. The unit uses AC mains or DC power supply of 12V to charge the accumulator. It can detect X-ray and gamma radiation from 15keV to 10MeV.

3.8.3 RDS-120 Universal Survey Meter

RADOS is the trade name of RDS-120 Universal Survey meter, used to detect gamma and X-ray of 50keV to 3MeV. It uses two energy compensated GM-tubes. It measures dose rate in the range of 0.01μSv to 10Sv.

3.9 CALCULATION OF THEORETICAL DETECTOR RESPONSE

Density of zircon sand = 2.5g/ml

Volume of zircon utilized = 19800ml

Therefore the mass of zircon used = 2.5 x 19800g = 49.5kg

Density of cement =1.7g/ml

Volume of cement = 9900ml

Therefore the mass of cement = (1.7 x 9980)g = 16.83kg

Total volume of source slab = 1x1x.03m³ = 0.03m³

Total activity of zircon slab per unit volume(S_v) = (specific activity of zircon x mass of zircon + specific activity of cement x mass of cement) divided by the volume of slab. is 0.0004563Ci/m^3

The total calculated detector response is R(P) = $\frac{2\pi S_v}{r^2} 193.8 \sum \frac{f_i E_i (\mu/\rho)_{air,i} e^{-\mu l}}{\mu}$ = 0.33432mR/h

3.9 CALCULATION OF EFFICIENCIES OF POINT SOURCES.

3.10 Efficiency Calibration

The efficiencies of the point sources were calculate using the formula

$$\varepsilon = \frac{(N - N_b)}{tAP_\gamma} e^{\frac{0.693\Delta t}{T_{1/2}}}$$

where N =counts in the peak at energy E

N_b = Background counts in the peak energy E

t =measurement live time (s)

A = activity of the prepared standard at the reference time stated in the certificate.

p_γ = Emission probability for gamma ray with energy E

Δt = time elapse since the reference time which is usually stated in the certificate

$T_{½}$ = Half-life of the radionuclide

Efficiency can be plotted against energy on a log-log diagram (IAEA, 1998)

Efficiency Calculation for Cs-137 (661.66keV),

Net count ($N-N_b$) = 251909counts

Δt =4488days

$T_{½}$ =10994.03days

P_γ =0.85

A= 37.92kBq

T = 100s

$$\varepsilon = \frac{(N - N_b)}{tAP_\gamma} e^{\frac{0.693\Delta t}{T_{½}}} = 7.8\%,$$

Efficiency Calulation for Co-60(1173.2keV),

Net count ($N-N_b$ = 41223counts

Δt = 4488days

$T_{½}$ = 1924.868 days

P_γ = 0.999

A= 48.27 kBq

T = 100s

$$\varepsilon = \frac{(N - N_b)}{tAP_\gamma} e^{\frac{0.693\Delta t}{T_{½}}} = 4.3\%,$$

Efficiency Calculation for Co-60(1332.5keV),

Net count $(N-N_b)$= 37216counts

Δt = 4488days

$T_{½}$ = 1924.868 days

P_γ = 0.99984

A= 48.27 kBq

T = 100s

$$\varepsilon = \frac{(N - N_b)}{tAP_\gamma} e^{\frac{0.693\Delta t}{T_{½}}} = 3.9\%,$$

These results obtained were used to plot the efficiency energy graph of figure 4.1.

CHAPTER FOUR

RESULTS AND DISCUSSION

4.0 INTRODUCTION

To achieve objectives stated in the introduction of this thesis various experiments were carried out. The results are as presented.

4.1 EFFCIENCY ENERGY GRAPH

Point sources of cesium137 and cobolt60 were used to acquire data using the NaI(Tl)detector the efficiencies were then calculated for the three energies as shown in section 3.10.

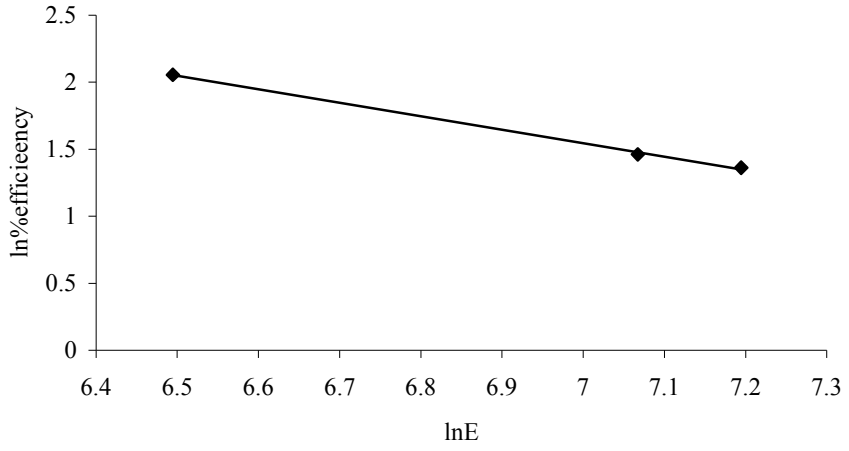

Figure 4.1 Efficiency against energy on natural log scale

Figure 4.1 shows the graph of percentage efficiency against photon energy on a log – log scale. The graph is a straight line, with efficiency decreasing with increasing energy. The equation of the line is y=-1.0053x +8.5802, where y represents the natural logarithm of percentage efficiency and x represents the natural logarithm of the photon energy in keV. The efficiencies of the three radionuclides of interest were calculated using the equation of the line and are as shown in table 4.1

Table 4.1 List of Radionuclide, Energy and Efficiency

Radionuclide	Energy(keV)	Efficiency(%)
Potassium (K)	1460	3.51
Radium	1764	2.90
Thorium	2614	1.95

The table above shows the efficiencies of K, Ra and Th, which were extrapolated from the efficiency-energy curve of point sources. The efficiency decreases with increasing energy.

The specific activity of standard, zircon sand and cement are as presented in Table 4.2. The specific activity were obtained by dividing the peak area of interest by the live time and mass, and then dividing the result obtained by the efficiency multiplied by a hundred. $\frac{(N - N_b)}{t \times m} \times \frac{100}{\eta} Bq / kg$

Table 4.2 Specific Activity of Standard, Zircon and Cement

	Standard (Bq/kg	Zircon (Bq/kg	Cement (Bq/kg
K	2030.098 ±137		23.124 ± 1.636
U	811.268 ± 106.95	538.848 ± 10.09	4.648 ± 1.446
Th	1585.276 ± 83.226	9726.151± 20.16	34.845 ± 1.655

The table indicates that the activity of thorium in the zircon is much higher than uranium while potassium was below the detection level. The activity due to the three radioelements is quite negligible in cement, while on the other hand the activity due to the presence of potassium in the standard is much higher than that of thorium and radium.

The concentration of the radionuclides of potassium, uranium and thorium in the standard were as stated in the IAEA document whilst the concentrations in zircon and cement were calculated by comparing their activities with that of the standard.

Table 4.3 Concentrations of Radionuclides in Standard, Zircon and Cement

	Standard	Zircon	Cement
K	44.8%	-	0.54%
U	400µg/g	265.69µg/g	2.3µg/g
Th	800µg/g	4908.2µg/g	17.6µg/g

The table shows that the concentration of thorium in the zircon sand is very much

higher than it is in the standard. The concentration of Th in the standard IAEA sample is 800ppm whilst the concentration of Th in the zircon sample used was 4808ppm. The concentration of Th in the sample is, therefore, six times that in the IAEA standard. The concentration of uranium in the standard is higher than in the zircon sand. The concentration of U in the IAEA standard is 400ppm while in the zircon sand used it is 266ppm. The K line was not present in the zircon sand sample used. The presence of the three radionuclides is very negligible in cement.

4.2 DISTRIBUTION OF RADIOACTIVITY OVER SLAB

The readings taken with the Ludlum GM tube and Scintillation detectors over the slab at seventeen varying slab-detector distance were in conformity with the inverse square law of radiation intensity. The readings at the periphery were lower than the readings at the centre; which showed that at the center the activity from the surrounding parts of the slab had a cumulative combining effect. The readings obtained at the same heights from different points showed that the radioactivity was uniformly distributed in the slab. Whilst the GM tube is sensitive to (α,β,γ) the Scintillation detector is sensitive only to γ particles and high energy β. Since the readings from both detectors are similar it indicated only gamma particles were being emitted.

Each distance of 12.5cm from the bottom left hand corner of the calibration pad was represented by 0.5units on the x-axis, while the y-axis is the count rate.

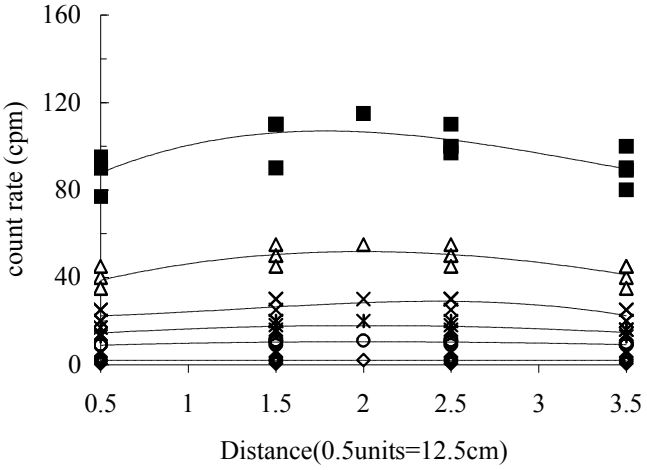

Figure 4.2 Distribution of activity over slab using Ludlum GM-Tube detector

The graph indicates that the activity close to the slab from the different positions is much higher. It also shows that the activity further away from the center is lower than those close to the center. This fact is more discernable for measurement close to the slab than those at higher distances.

The topmost curve is the readings obtained at a height of 5cm from the slab, the second one is that obtained at a height of 25cm from the slab, the others are at 50cm, 75cm and 100cm respectively from the slab. The graphs at 100cm and 75cm show that the there is no variations at these distances regardless of where the readings were taken. The solid angle effect can be deduced from the result because at the center the detector captures more of the photons.

The figure 4.3 shows distribution of dose rate on the pad. 0.5 units on the x-axis represents 12.5cm on the calibration pad starting from the bottom left hand corner. The y-axis is the dose rate.

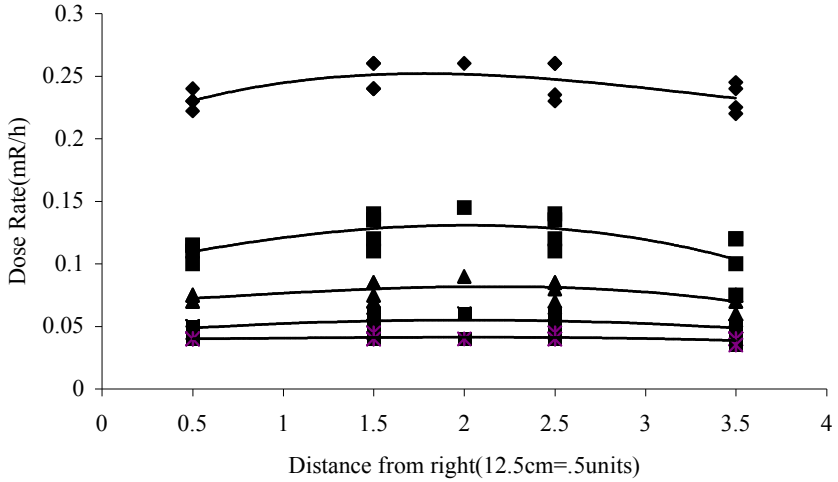

Figure 4.3 Measured dose rate distribution over slab using Ludlum NaI(Tl) detector

The graph has been plotted to fit a third degree polynomial, as it is a three-parameter graph. The graph is that of dose rate against that height at different positions from the slab, using Ludlum NaI(Tl) detector. It is obvious the observation made with Ludlum GM tube is the same as that obtained with the NaI(Tl).

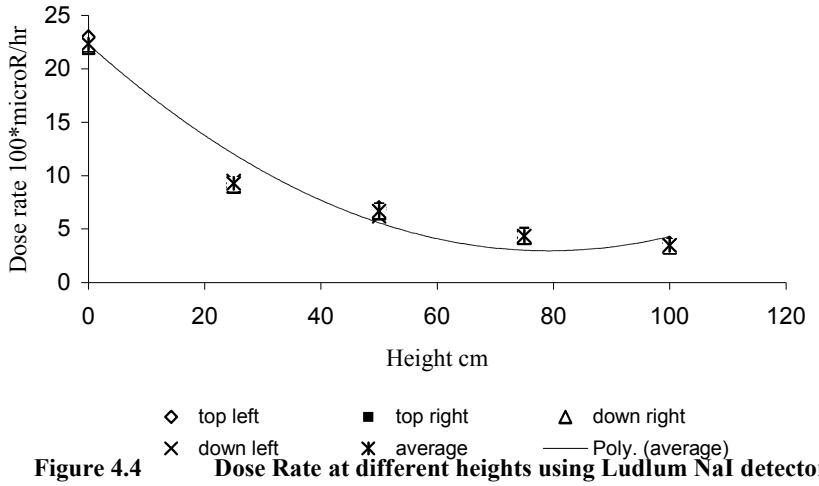

Figure 4.4 Dose Rate at different heights using Ludlum NaI detector

Graph of dose rate against height above slab at four edges of the pad, using NaI(Tl) (Ludlum) portable detector. The readings obtained at the same height from the different corners were almost the same showing that the activity is uniformly distributed at equidistant points from the center of the pad. The readings also showed the inverse law of reducing radiation intensity with increasing distance from pad

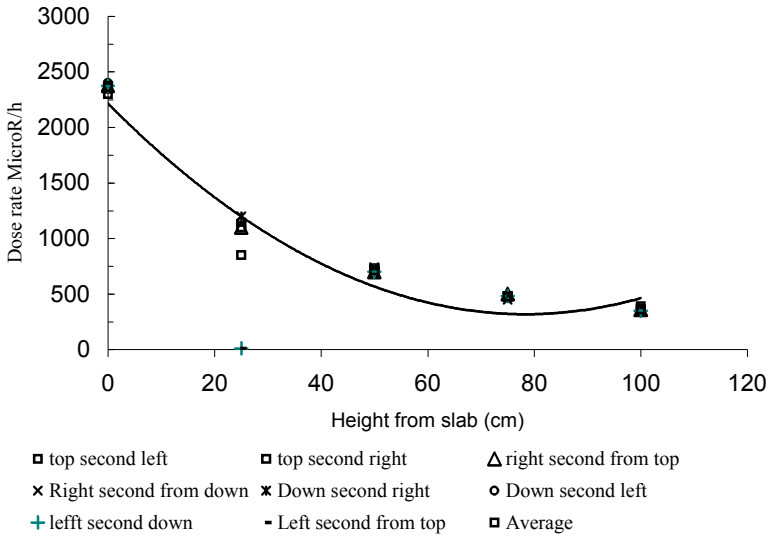

Figure 4.5 Dose Rate against height at eight equidistant positions from the center of slab

The positions indicated in figure 4.5 are with respect to the partitioning of the pad as shown in Figure 3.3. The readings at the eight different positions from the center, which are actually at equidistant positions, are identical, confirming the uniform distribution of radiation intensity. The readings were also a bit higher than that obtained at the edges of the slab.

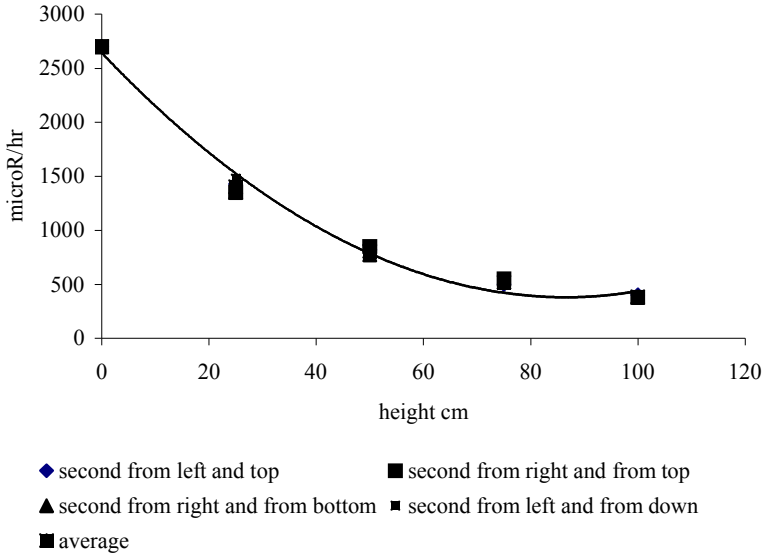

Figure 4.6 Activity against height at four equidistant positions from the center

Graph of dose rate against height from pad at the four points shown, are actually equidistant points from The concentration of Th in the standard IAEA sample the centre of the pad. The readings were obtained using Ludlum NaI hand held detector. The readings were indicative of the inverse square rule and the solid angle effect of reducing radiation intensity with increasing distance from the source. The readings were also a bit higher than that obtained at the edges and that of the eight equidistant positions, as they are closer to the center. The readings obtained from the four different points are infact the same hence the points overlap.

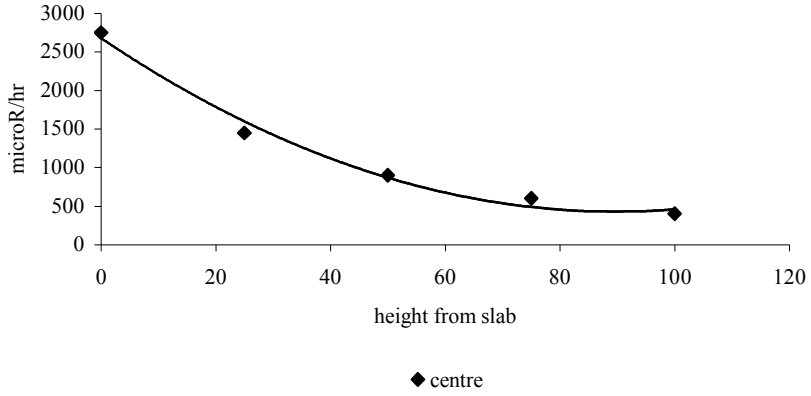

Figure 4.7 Activity against height over center of slab

The highest readings were obtained at the center showing the cumulative effect of the radiation intensity from the other sections of the slab. This is also due to the solid angle

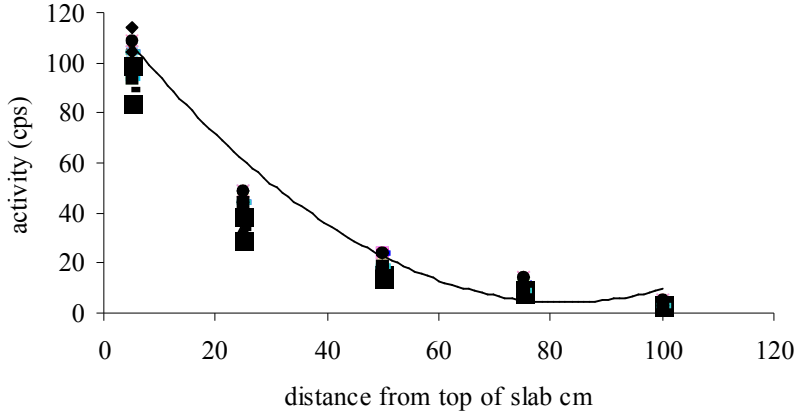

Figure 4.8 Graph of activity against distance

The activity measured at seventeen different positions, the centers of the gridded pad at five heights using LUDLUM GM-Tube portable detector. The readings show that the activity from equidistant positions from the center actually overlaps, which confirms the uniform distribution of activity over the slab

4.3 CALIBRATION CURVES

The calibration curves, which are the calculated dose rate against measured dose rates or activity, are as presented in the following graphs

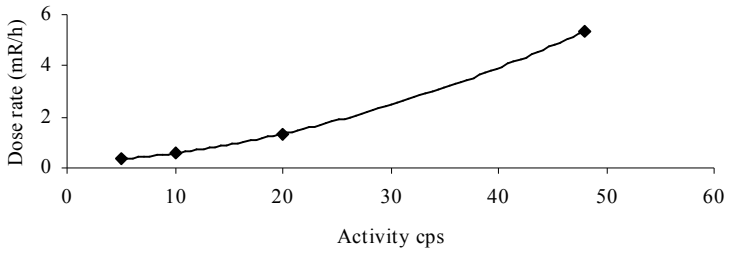

Figure 4.9 Calibration Curve Calculated Dose Rate vs Measured Activity with GM-Tube

.

The calculated dose rate against measured activity using Gm-tube is not a straight-line relationship between the range of 25cm to 100cm.. The graph obtained is a second-degree polynomial relationship for the range of distance chosen. The fit equation is $y = 0.0018x^2 + 0.0224x + 0.1835$

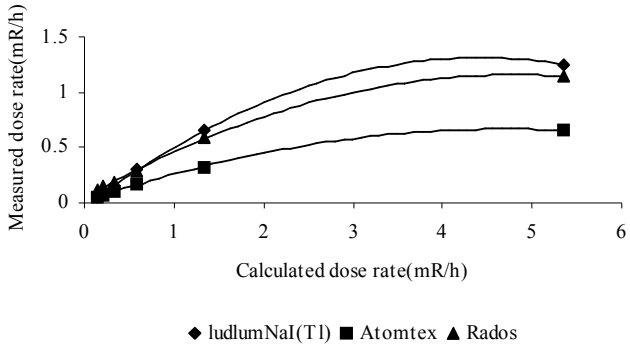

Figure 4.10 Calculated versus Measured Dose Rate

The graph shows that the calculated dose rate is much higher than the measured dose rate since it is not possible for any detector to detect and register all the photons being emitted by a radionuclide. It is not a straight-line graph because dose rate very close to the slab diverges due to geometrical factor and because the equation used for the analytical calculation is divided by inverse of distance squared.

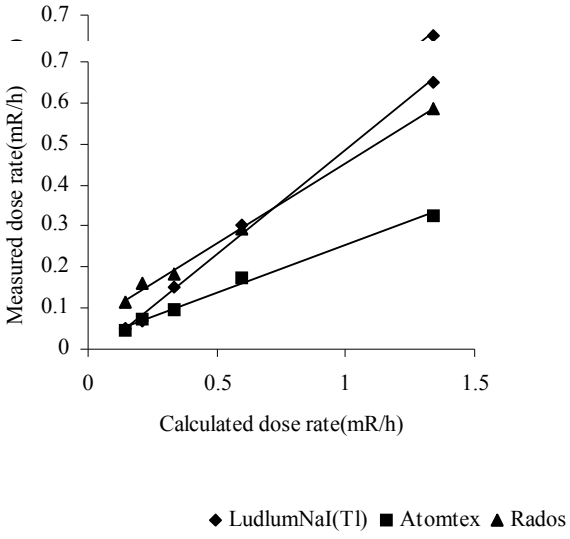

Figure 4.11 Calibration curve

The three curves are the calibration curves obtained using NaI (LUDLUM), Energy compensated GM-Tubes(RADOS)and Plastic scintillator (ATOMTEX) portable survey meters respectively. The range chosen to give the straight-line graphs was between 25cm and 150 cm. The equations of the straight lines obtained are as follows. y=0.5096x-0.0239 for NaI(Tl), the intercept is on the negative Y-axis.

y = 0.233x+0.0203 for ATOMTEX and

y = .39x + 0.062 for RADOS detectors respectively where y represents the measured dose rate and x the calculated dose rate. The efficiency of Sodium iodide detector is a bit over 50%, above 23% for Atomtex and 39% for Rados detector. These three detectors can be calibrated between 25 and 150cm.

4.4 COMPARISON WITH INTERNATIONAL STANDARDS

The recommended IAEA dimension of Calibration Pad for Portable Detectors is (1x1x0.3)m^3 but the dimension of the calibration pad used in this work is (1x1x0.03)m^3.

The IAEA recommends at least four pads as follows:

Pad one spiked with 8% potassium, Pad two spiked with 50ppm Uranium, Pad three spiked with 125ppm Thorium and Pad four is the control with no added radionuclide. In this work only one pad was used and it was spiked with zircon sand. The concentration of the zircon sand used was 265ppm uranium and 9726ppm thorium as determined in the laboratory, the concentration of radionuclides is therefore higher than the IAEA recommendation. The calculated total detector response is 0.33432mR/h while the highest measured dose rate was 2.5μR/h. The calibration or conversion factor was obtained by plotting readings obtained with portable detectors with that calculated analytically. Hence the conversion factor obtained in this work is a ratio and therefore, dimensionless, whilst the calibration factor obtained from previous work is given in cps/pCi/g and for each of the three radioelements. In this work `the background was taken at a distance of 1m from the pad, instead of using an unspiked pad (control) for background readings.

4.5 SUMMARY

This work has confirmed previous works by other researchers, which found that the activity of the tailing from the tin mining area is mainly due to thorium. The concentration of potassium is below the detection level in the zircon sand used, while the concentration of Radium-226 is 538.848±10.09Bq/kg and that of thorium is 9726.151±20.16 Bq/kg. The activity cement is in fact negligible. The concentrations of potassium, radium and thorium are 23.124±1.535 Bq/kg, 4.648±1.446Bq/kg and34.845±1.655Bq/kg respectively. The inverse square law with increasing distance was also confirmed by this investigation. It was also found that the radioactivity was uniformly distributed over the slab with points of equidistant positions from the center of the slab giving identical values of dose rates. The highest reading of dose rate is obtained at center of the slab, which can be attributed to the contribution from surrounding parts of the pad and the solid angle effect. The calibration curve is a straight line between the ranges of 25cm and150cm; hence the result obtained can be comfortably used within this range. This work also indicates that the efficiency of sodium iodide detector is higher than the others used.

Table 4.4 Calibration Factors

Detector	Calibration Factor
LUDLUM NaI (Tl)	0.5096
ATOMTEX	0.233
RADOS	0.39

CHAPTER FIVE

CONCLUSION AND RECOMMENDATIONS

5.1 CONCLUSION

This study has shown that it is possible to locally construct calibration slab using highly radioactive tailings of zircon sand from the Tin mines, which is available and cheap. The activity of the zircon sand was mainly due to the presence of thorium. Usually detectors are calibrated using detectors, which have been calibrated with primary detectors that is by comparing readings of radiation intensity of the secondary detector with that of the readings obtained with the detector being calibrated but due to the unavailability of secondary detectors pad has been used for calibration. Infact it is standard practice to calibrate detectors meant for environmental measurements with calibration pad. Calibration pad is meant to simulate the environment in which the detector is be used hence the concrete is usually spiked with known amount of potassium, uranium and thorium, the three main naturally occurring radionuclides. In this work zircon, which, is known to contain a very high concentration of thorium, has been used to construct the pad hence zircon was characterized to ascertain its activity. From the readings obtained of uniform radiation intensity from equidistant positions, it shows that the cement and zircon sand were thoroughly mixed and hence the uniform activity. The radiation dose sloped gently towards the edges of the slab and peaked towards the center. Theoretical expected dose rates using formula for volume sources was compared with the readings obtained with detectors for environmental measurement. Straight-line graphs were obtained when the calculated dose rates were plotted against measured dose rates, as shown in figure 4.11.The calibration factors, which are the slopes of the three graphs, are as tabulated in table 4.4

5.2 RECCOMMENDATION

For optimum results it will be advisable that future work should be carried out using different concentrations of the zircon sand to construct several slabs and one pad with no added zircon to serve as the control pad for background measurements.

In future work it is recommended that the concentration of each of the three naturally occurring radioelements be determined after constructing the pad to simplify computation of the conversion factors

REFERENCES

A.bdulrashid, F. I. (2000) "Comparison of Some Nigerian Cements for Low Level Radioactive Waste Conditioning", MSc Thesis, Ahmadu Bello University pp 51.

Adams, F. and Dams, R. (1975) *"Applied Gamma Ray Spectrometry"* Pergamon Press New York pp45-46

Agbazue, V. E. (1992) "*A guide to Cement Industry and quality control in Nigeria"*, Fourth Dimension Publishing Company Ltd Enugu Nigeria pp.52.

Ajayi, I. R. Oresegon, M.O &. Babalola, I.A (1996) "Absorbed dose Rates in Air due to U, Th & K in a Part of South Western Nigeria", *Nigerian Journal of Physics*, Vol 8, pp38

Ajayi,I.R.,Ajayi, O.S. and Fasuyi, O.S(1995)"The Natural Radioactivity of Surface Soil in Ijero-Ekiti", *Nigerian Journal of Physics* Vol7, pp101

Alan, M. and Harbison, S.A (1988) *"An Introduction to Radiation Protection"*, J. W. Arrow Smith Ltd, Bristol, pp8-14

Burcharm, W. E. (1963) *"Nuclear Physics- An Introduction"*, Longman Green and Co Ltd. pp194-204.

Cember H. (1992). *"Introduction to Health Physics*" McGraw-Hill, Inc USA. pp79-123

Dewu, B.B.M."Uranium Series Disequilibrium Investigation on Granite and Granite related Materials on the Jos Plateau" *Nigerian Journal of Physics* Vol5, pp87

George R.W.and Raymond J.P.(1980) *"Principles of Quality Concrete*" Portland Cement Association John Wiley and Sons,INC.Canada pp168-169

Grasty, R.L., Holman, P.B, Blanchard, Y.(1991) "Transportable Calibration Pads for Ground and Airborne Gamma Ray Spectrometry" *Geol. Survey can paper*

Hendee W. R. and Ibbott, G. S. (1996) *"Radiation Therapy Physics"*, Mosby – Yearbook Inc. USA. pp10-15

IAEA (1990)- *"The Use of Gamma Ray Data to Define the Natural Radiation Environment"*, TECDOC-566 International Atomic Agency Vienna, pp 8, 16-19.

IAEA (1990). *"Practical Aspects of Operating a Neutron Activation Analysis Laboratory"*, TECDOC-564. International Atomic Energy Agency, Vienna. pp 58-65

IAEA, (1999) *"Generic Procedure in Nuclear or Radiological Emergency"*. TEC-DOC 1092 International Atomic Agency Vienna pp146-148, 254-256

IAEA, (2003) *"Guidelines for Radioelement mapping using Gamma Ray Spectrometry Data"*, TECDOC 1363 pp5, 34-35.

Ibeanu, I.G.E. (1999) "Assessment of Radiological effects of the Mining Activities in Jos and its Environs". PhD Thesis Ahmadu Bello University Zaria.pp 69,73-77,83-99

ICRP (1990) *Recommendations of the International Commission on Radiological Protection.* Annals of ICRP-60, Pergamon Press Oxford.pp25

Janssen A. and Linsley, G. (1998) "Proceedings of Second International Symposium on the Treatment of Naturally Occurring Radioactive Materials", Krefeld-Germany pp32-41

Karl Z. M and James E. T (1967) *"Health Physics"*, Oak Ridge Tennessee McGraw-Hill, Inc USA pp282-293

Khan, F.M. (1992). *The Physics of Radiation Therapy John Wiley and Sons England. pp*425

Kidder – Parker (1968) *"Architect's & Builders Handbook, Data for Architects, Structural Engineers Contractors and Draughtsman"*, 18th edition John Wiley & Sons, Inc New York.pp 6(224)

Knoll, G.F. (1989). *"Radiation Detection and Measurement*" John Wiley and Sons, Inc. Canada. pp.388-417

Microsoft Encarta Encyclopedia (2002)"Radiation"

Nias A.W.H. (1990) "An Introduction to Radiobiology" John Wiley & Sons Ltd England. pp311

Price, W.J.(1967) *"Nuclear Radiation Detection"* McGraw –Hill Series in Nuclear Engineering Thomas H.Pigford Consulting Editor pp192-235

Rabi'u. N. (1993) "Radioactivity Level Around the Jos Tin Mines Area" MSc Thesis Ahmadu Bello University pp46-49

Sharpe, J.(1955) *"Nuclear Radiation Detectors"*.W.S.Cowell Ltd Ipswich, Britain pp 2-5

Singru R. M. (1972) *"Introduction to Experimental Nuclear Physics"*, Wiley Eastern Private Ltd New Delhi pp44-54

Tait W. H. (1980) *"Radiation Detection"* Butterworth & Co (Publishers) Ltd London pp107-156

Tsoulfanidis, N. (1983) *"Measurement and Detection of Radiation"*. Hemisphere Publishing Corporation N.Y pp247-251